MATHEMATICS OF COMPUTATION
Volume 00, Number 0, Pages 1–19
S 0025-5718(XX)0000-0

STABILITY OF THE VARIABLE TWO-STEP BDF SCHEME FOR PARABOLIC EQUATIONS UNDER A SHARP RATIO CONDITION

GEORGIOS AKRIVIS, YIFAN WEI, JIWEI ZHANG, AND CHENGCHAO ZHAO

Abstract. We consider the discretization of linear parabolic equations with selfadjoint elliptic part by the variable-step two-step BDF method. We establish stability estimates, analogous to the standard stability estimate for the continuous problem, under a sharp condition on the ratios of adjacent time-steps, namely, under the well-known sharp ratio condition for the zero-stability of the scheme. We also present results of numerical experiments that validate the theoretical findings.

1. Introduction

Let $T > 0, u_0 \in H$, and consider the initial value problem of seeking $u \in C((0,T];\mathscr{D}(A)) \cap C([0,T];H)$ satisfying

$$\begin{cases} u'(t) + Au(t) = f(t), \quad 0 < t < T, \\ u(0) = u_0, \end{cases} \tag{1.1}$$

with A a positive definite, selfadjoint, linear operator on a Hilbert space $(H, (\cdot,\cdot))$, with domain $\mathscr{D}(A)$, and $f : [0,T] \to H$ a given forcing term.

The backward difference formula (BDF) methods are popular for stiff differential equations, in particular, for parabolic equations. They are frequently implemented on nonuniform partitions for numerical efficiency.

For an integer $N \geqslant 2$, consider a partition $0 = t_0 < t_1 < \cdots < t_N = T$ of the time interval $[0,T]$, with time steps $\tau_n := t_n - t_{n-1}, n = 1,\dots,N$. We recursively define a sequence of approximations u^n to the nodal values $u(t_n)$ of the exact solution by the variable two-step BDF method,

$$\dot{u}^n + Au^n = f^n, \quad n = 2,\dots,N, \tag{1.2}$$

with $f^n := f(t_n)$, assuming that arbitrary starting approximations $u^0, u^1 \in H$ are given. Here, with $r_n := \tau_n/\tau_{n-1}, n = 2,\dots,N$, the adjacent time-step ratios, the

Received by the editor October 21, 2025, and, in revised form, November 15, 2025, and April 24, 2026.

2020 *Mathematics Subject Classification.* 65M06, 35B65.

Key words and phrases. Variable-step, two-step BDF method, parabolic equations, stability, sharp ratio condition.

This work was supported by the National Natural Science Foundation of China under grant No. 12571438 and the Fundamental Research Funds for the Central Universities 2042021kf0050.

discrete time derivative $\dot{v}^n$ associated with the two-step BDF method is given by

$$\dot{v}^n := \frac{1+2r_n}{(1+r_n)\tau_n}(v^n - v^{n-1}) - \frac{r_n^2}{(1+r_n)\tau_n}(v^{n-1} - v^{n-2}), \quad n = 2, \dots, N. \tag{1.3}$$

Let $|\cdot|$ denote the norm on H induced by the inner product $(\cdot,\cdot)$. We identify H with its dual and denote by V' the dual of $V, V := \mathscr{D}(A^{1/2})$. We introduce on V the norm $\|\cdot\|$ by $\|v\| := |A^{1/2}v|$ and on V' the dual norm $\|\cdot\|_\star$ by $\|v\|_\star = |A^{-1/2}v|$. We shall use the notation $(\cdot,\cdot)$ also for the antiduality pairing between V' and V. For simplicity, we denote by $\langle\cdot,\cdot\rangle$ the inner product on V, $\langle v,w\rangle := (A^{1/2}v, A^{1/2}w)$.

1.1. **Main result.** We establish the following stability result.

Theorem 1.1 (Stability of the variable two-step BDF method)**.** *Let $u^n \in V$ satisfy (1.2), with $u^0, u^1 \in H$, and assume that*

$$r_i = \frac{\tau_i}{\tau_{i-1}} \leqslant r^\star < 1 + \sqrt{2}, \quad i = 2, \dots, N. \tag{1.4}$$

Then, the variable two-step BDF method (1.2) is stable in the sense that

$$|u^n|^2 + \sum_{\ell=2}^{n} \tau_\ell \|u^\ell\|^2 \leqslant C\Big(|u^0|^2 + |u^1|^2 + \sum_{\ell=2}^{n} \tau_\ell \|f^\ell\|_\star^2\Big), \quad n = 2, \dots, N. \tag{1.5}$$

Here, C denotes a generic constant, depending only on the upper bound $r^\star$ of the adjacent step ratios r_i, independent of T and the operator A as well as of f and of the step sizes τ_i.

The condition on $r^\star$ in (1.4) is sharp, in the sense that for $r^\star \geqslant 1 + \sqrt{2}$ the stability estimate (1.5) is, in general, not valid. However, (1.5) may be valid if (1.4) is violated, for instance, if only a fixed number $n^\star$, independent of N, of ratios r_i exceed the upper bound $1 + \sqrt{2}$.

Let us note that (1.5) is a discrete analogue of the standard stability estimate for the continuous problem (1.1),

$$|u(t)|^2 + \int_0^t \|u(s)\|^2 \,\mathrm{d}s \leqslant |u_0|^2 + \int_0^t \|f(s)\|_\star^2 \,\mathrm{d}s, \quad 0 < t \leqslant T. \tag{1.6}$$

1.2. **Previous work.** Stability of the A-stable two-step BDF method for parabolic equations for equidistant partitions can be easily established by the energy technique. The zero-stability property, and thus the stability for o.d.e's satisfying the Lipschitz condition, of the variable two-step BDF method is also well understood; a sufficient condition is (1.4) and the bound is sharp; see [5, 9] as well as [12, p. 405].

Grigorieff proved stability for parabolic equations for $r^\star \leqslant (1+\sqrt{3})/2 \approx 1.366$ in [10, 11]. In [2, 3], Becker established stability analogous to (1.5) for linear parabolic equations for $r^\star \leqslant (2 + \sqrt{13})/3 \approx 1.8685$; see also [16, pp. 174–180]. Emmrich [8] relaxed the bound to 1.9104 for semilinear parabolic equations. More recently, the bound was further slightly relaxed to 1.9398 for linear parabolic equations in [1]. Let us also mention that in [1, 3, 8, 16] an additional condition is required, namely, that the mesh-dependent quantities $\varGamma_n$,

$$\varGamma_n := \sum_{i=2}^{n-2} [r_i - r_{i+2}]_+ \quad \text{with} \quad [x]_+ := \max(x, 0),$$

be bounded.

Here, we considerably relax the bound and establish the standard stability estimate (1.5) for linear parabolic equations under the sharp zero-stability condition $r^\star < 1+\sqrt{2}$.

Stability estimates of a different kind, in which the difference quotient $(u^1 - u^0)/\tau_1$ enters into the right-hand side, have also been established for linear as well as for nonlinear parabolic equations, for bounds $r^\star$ significantly larger than the optimal bound $1+\sqrt{2}$ for zero-stability; see [6, 7, 14, 17–20] and references therein. Notice that $(u^1 - u^0)/\tau_1$ may enter implicitly in such estimates, through f^1, for instance, if the starting value u^1 is computed by employing one step of the implicit Euler method. An example with uniformly bounded $|u^0|$ and $|u^1|$ but not uniformly bounded $|(u^1-u^0)/\tau_1|$ is $u^1 := (1+\alpha\tau_1)u^0 + v$ with a real number α and a nonzero $v \in H$.

Let us comment on the discrepancy of the conditions that are required for the two kinds of stability estimates. In the case of the test equation $u' = 0$ in the interval $[0, T]$, with starting values $u^0, u^1, u^1 \neq u^0$, and for constant ratios r, i.e., for $\tau_n = \tau_1 r^{n-1}, n = 1, 2, \dots,$ the method reads

$$u^n - u^{n-1} = \alpha_1(u^{n-1} - u^{n-2}) \quad \text{or} \quad \bar\partial u^n = \alpha_2 \bar\partial u^{n-1}, \quad n = 2, \dots, \tag{1.7}$$

with the backward difference quotients $\bar\partial v^n := (v^n - v^{n-1})/\tau_n$ and the amplification factors

$$\alpha_1 := \frac{r^2}{1+2r} = r\alpha_2 \quad \text{and} \quad \alpha_2 := \frac{r}{1+2r}.$$

Now, the second amplification factor, α_2, is less than $1/2$ for any r, whence

$$|\bar\partial u^n| \leqslant \frac{1}{2}|\bar\partial u^{n-1}| \quad \text{and thus} \quad |\bar\partial u^n| \leqslant \frac{1}{2^{n-1}}|\bar\partial u^1|.$$

The latter relation leads easily to

$$|u^n| \leqslant |u^1| + \sum_{\ell=2}^{n} \frac{\tau_\ell}{2^{\ell-1}} \cdot |\bar\partial u^1|, \quad n = 2, \dots, N,$$

and thus to a (nonstandard) stability estimate of the form

$$|u^n| \leqslant |u^1| + \max_{2 \leqslant \ell \leqslant n} \tau_\ell \cdot |\bar\partial u^1|, \quad n = 2, \dots, N. \tag{1.8}$$

In contrast, the first relation in (1.7) yields $u^n - u^{n-1} = \alpha_1^{n-1}(u^1 - u^0)$, and thus

$$u^n = u^1 + \sum_{\ell=1}^{n-1} \alpha_1^\ell \cdot (u^1 - u^0), \quad n = 2, \dots, N.$$

We easily see that the stability estimate

$$|u^n| \leqslant |u^1| + C|u^1 - u^0|, \quad n = 2, \dots, N, \tag{1.9}$$

is valid if and only if the amplification factor α_1 is less than 1, i.e., if and only if $r < 1+\sqrt{2}$.

The numerical examples in Section 5 confirm that for a fixed ratio $r > 1+\sqrt{2}$, the numerical approximations at $t = T$ blow up as $N \to \infty$, while for $r < 1+\sqrt{2}$, the boundedness of the numerical approximations is preserved independently of N.

BDF methods are popular for stiff equations, in particular, for parabolic equations. They have good damping properties, do not suffer from order reduction, and require at every time level only the solution of an equation (system) of the form of the implicit Euler method, and are, thus, computationally efficient.

An outline of the article is as follows: We establish key auxiliary results in Section 2 and provide the proof of Theorem 1.1 in Section 3. In Section 4, we extend our stability analysis to the case of nonautonomous equations and in Section 5 we present results of numerical experiments.

2. Auxiliary results

As a preparation for the proof of Theorem 1.1, which we give in the next section, we present here auxiliary results. The proof of Theorem 1.1 mainly utilizes properties of the DOC and DCC kernels from [6, 13, 14, 18, 19], supplemented by a new key estimate for the DCC kernels. Accordingly, this section is structured as follows: in Section 2.1, we introduce notation; pertinent properties of the DOC and DCC kernels are recalled in Section 2.2; in Section 2.3, we establish a novel critical estimate for the DCC kernels. Finally, in Section 2.4, we give a discrete Gronwall-type inequality.

2.1. **Notation.** For notational convenience, we introduce also the discrete time derivative $\dot v^1 := (v^1 - v^0)/\tau_1 = \bar\partial v^1$ for $n = 1$. With the notation $b_0^{(1)} := 1/\tau_1$ and, for $n > 1$,

$$b_0^{(n)} := \frac{1+2r_n}{(1+r_n)\tau_n},\quad b_1^{(n)} := -\frac{r_n^2}{(1+r_n)\tau_n},\quad \text{and}\quad b_i^{(n)} = 0,\quad i = 2,\dots,n-1, \tag{2.1}$$

for the BDF coefficients, the discrete time derivatives can be written in a discrete convolution form,

$$\dot v^n = \sum_{k=1}^n b_{n-k}^{(n)}(v^k - v^{k-1}),\quad n = 1,\dots,N. \tag{2.2}$$

The *discrete complementary convolution* (DCC) kernels $p_i^{(n)}$ are defined by

$$\sum_{i=k}^n p_{n-i}^{(n)} b_{i-k}^{(i)} = 1,\quad k = 1,\dots,n,\quad n = 1,\dots,N; \tag{2.3}$$

see [18]. This definition is motivated by the fact that it leads to a discrete analogue of the fundamental theorem of calculus, $\int_0^t v'(s)\,\mathrm{d}s = v(t) - v(0)$; more precisely,

$$\begin{aligned}\sum_{i=1}^n p_{n-i}^{(n)}\dot v^i &= \sum_{i=1}^n p_{n-i}^{(n)}\sum_{\ell=1}^i b_{i-\ell}^{(i)}(v^\ell - v^{\ell-1}) = \sum_{\ell=1}^n (v^\ell - v^{\ell-1})\sum_{i=\ell}^n p_{n-i}^{(n)} b_{i-\ell}^{(i)}\\ &= \sum_{\ell=1}^n (v^\ell - v^{\ell-1}),\end{aligned}$$

whence

$$\sum_{i=1}^n p_{n-i}^{(n)}\dot v^i = v^n - v^0,\quad n = 1,\dots,N. \tag{2.4}$$

The *discrete orthogonal convolution* (DOC) kernels $\theta_i^{(n)}$ are defined by

$$\sum_{i=k}^n \theta_{n-i}^{(n)} b_{i-k}^{(i)} = \delta_{nk},\quad k = 1,\dots,n,\quad n = 1,\dots,N, \tag{2.5}$$

with δ_{nk} the Kronecker delta symbol; see [14]. These kernels play a key role in our analysis. It follows immediately from this definition that

$$\sum_{i=1}^{n}\theta_{n-i}^{(n)}\dot v^i=\sum_{\ell=1}^{n}(v^\ell-v^{\ell-1})\sum_{i=\ell}^{n}\theta_{n-i}^{(n)}b_{i-\ell}^{(i)}=\sum_{\ell=1}^{n}\delta_{n\ell}(v^\ell-v^{\ell-1})$$

and thus

$$\sum_{i=1}^{n}\theta_{n-i}^{(n)}\dot v^i=v^n-v^{n-1},\quad n=1,\dots,N. \tag{2.6}$$

The DOC kernels $\theta_i^{(n)}$ and the DCC kernels $p_i^{(n)}$ are related as follows (see [18]),

$$p_{n-i}^{(n)}=\sum_{\ell=i}^{n}\theta_{\ell-i}^{(\ell)},\quad i=1,\dots,n. \tag{2.7}$$

2.2. **Positive-definiteness of the DOC kernels $\boldsymbol{\theta_i^{(n)}}$.** We revisit here the positive definiteness of the DOC kernels and some properties of both the DCC and DOC kernels. The positive definiteness of the DOC kernels was established in [6, Lemma 2.5] under the ratio condition $r_k<4.8645$, with its proof relying on the positive definiteness of the BDF kernels as shown in [19]. Related work on the positive definiteness of the BDF kernels can be found in [4, 13, 14, 18, 20].

For the sake of completeness, we here prove the positive definiteness of both, the BDF kernels $b_i^{(n)}$ and the DOC kernels $\theta_i^{(n)}$, under the ratio condition $r_k\leqslant r_\star:=1+\sqrt{2}$; this more stringent condition leads to sharper lower bounds.

Consider the lower bidiagonal $n\times n$ matrix B and its inverse $\Theta:=B^{-1}$ (see [6, 7, 13])

$$B:=\begin{pmatrix} b_0^{(1)} & & & 0\\ b_1^{(2)} & b_0^{(2)} & & \\ & \ddots & \ddots & \\ 0 & & b_1^{(n)} & b_0^{(n)}\end{pmatrix}\quad\text{and}\quad \Theta:=\begin{pmatrix} \theta_0^{(1)} & & & 0\\ \theta_1^{(2)} & \theta_0^{(2)} & & \\ \vdots & \ddots & \ddots & \\ \theta_{n-1}^{(n)} & \cdots & \theta_1^{(n)} & \theta_0^{(n)}\end{pmatrix}$$

as well as the diagonal matrix $\mathcal{T}:=\operatorname{diag}(\sqrt{\tau_1},\dots,\sqrt{\tau_n})$. Notice that the relation $\Theta=B^{-1}$ is an immediate consequence of (2.5). In the following auxiliary results we shall use the notation $(\cdot,\cdot)$ and $\|\cdot\|$ for the Euclidean inner product and the associated norm on $\mathbb{R}^n$.

Lemma 2.1 (Positive definiteness of B)**.** *Assume that the time step ratios r_k are such that $r_k\leqslant r_\star=1+\sqrt{2}$. Then, the matrix B is positive definite; more precisely,*

$$(Bv,v)\geqslant\frac{1}{2}\|\mathcal{T}^{-1}v\|^2\quad\forall v\in\mathbb{R}^n. \tag{2.8}$$

Proof. Using the binomial inequality $2ab\leqslant a^2+b^2$ and the fact that $b_1^{(k)}<0$, we have, for $k\geqslant 2$,

$$2v_k\sum_{i=1}^{k}b_{k-i}^{(k)}v_i=2b_0^{(k)}v_k^2+2b_1^{(k)}v_kv_{k-1}\geqslant\left(2b_0^{(k)}+b_1^{(k)}\right)v_k^2+b_1^{(k)}v_{k-1}^2,$$

i.e.,

$$2v_k\sum_{i=1}^{k}b_{k-i}^{(k)}v_i\geqslant\frac{2+4r_k-r_k^2}{1+r_k}\frac{v_k^2}{\tau_k}-\frac{r_k}{1+r_k}\frac{v_{k-1}^2}{\tau_{k-1}}. \tag{2.9}$$

Now, as we shall see,

$$\frac{2+4x-x^2}{1+x} \geqslant 1 + \frac{y}{1+y} \quad \forall x, y \in [0, r_\star], \tag{2.10}$$

and thus, choosing $x = r_k$ and $y = r_{k+1}$, (2.9) yields the preliminary estimate

$$2v_k \sum_{i=1}^{k} b_{k-i}^{(k)} v_i \geqslant \Big(1 + \frac{r_{k+1}}{1+r_{k+1}}\Big)\frac{v_k^2}{\tau_k} - \frac{r_k}{1+r_k}\frac{v_{k-1}^2}{\tau_{k-1}}, \quad k \geqslant 2. \tag{2.11}$$

To see (2.10), since $y/(1+y)$ is increasing, it suffices to show that

$$\varphi(x) \geqslant 1 + \frac{r_\star}{1+r_\star} \quad \forall x \in [0, r_\star] \tag{2.12}$$

with φ the rational function $\varphi(x) := (2+4x-x^2)/(1+x)$. This relation is obvious for $x = 0$ since $\varphi(0) = 2$, and it holds as equality for $x = r_\star$. Furthermore,

$$\varphi'(x) = -\frac{x^2+2x-2}{(1+x)^2},$$

whence φ is increasing in $[0, \sqrt{3}-1]$ and decreasing in $(\sqrt{3}-1, r_\star]$. We thus infer that φ attains its minimum in $[0, r_\star]$ at $r_\star$, and (2.12) is valid for every $x \in [0, r_\star]$.

Now, we sum up (2.11) from $k = 2$ to $k = n$, and get

$$2\sum_{k=2}^{n} v_k \sum_{i=1}^{k} b_{k-i}^{(k)} v_i \geqslant \sum_{k=2}^{n} \frac{v_k^2}{\tau_k} + \frac{r_{n+1}}{1+r_{n+1}}\frac{v_n^2}{\tau_n} - \frac{r_2}{1+r_2}\frac{v_1^2}{\tau_1}, \quad n = 2, \dots, N.$$

Ignoring the second term on the right-hand side and adding

$$2v_1 b_0^{(1)} v_1 = 2\frac{v_1^2}{\tau_1} \geqslant \Big(1 + \frac{r_2}{1+r_2}\Big)\frac{v_1^2}{\tau_1} \tag{2.13}$$

to both sides, we obtain

$$2(Bv, v) = 2\sum_{k=1}^{n} v_k \sum_{i=1}^{k} b_{k-i}^{(k)} v_i \geqslant \sum_{k=1}^{n} \frac{v_k^2}{\tau_k} = \|\mathcal{T}^{-1}v\|^2, \quad n = 2, \dots, N. \tag{2.14}$$

In view of (2.13), (2.14) is valid also for $n = 1$. The proof is complete. ☐

We next prove [6, Lemma 2.5] under the ratio condition $r_k \leqslant r_\star = 1 + \sqrt{2}$ in the following Lemma.

Lemma 2.2 (Positive definiteness of Θ)**.** *For time step ratios such that $r_k \leqslant r_\star = 1 + \sqrt{2}$, the matrix Θ is positive definite; more precisely,*

$$(\Theta v, v) \geqslant \frac{1}{20}\|\mathcal{T}v\|^2 \quad \forall v \in \mathbb{R}^n. \tag{2.15}$$

Proof. Let us consider the symmetric parts B_s and Θ_s of B and Θ,

$$B_s = (B + B^\top)/2, \quad \Theta_s = (\Theta + \Theta^\top)/2.$$

Then, (2.15) can be equivalently written in the form

$$(\Theta_s v, v) \geqslant \frac{1}{20}\|\mathcal{T}v\|^2 \quad \forall v \in \mathbb{R}^n. \tag{2.16}$$

In view of the obvious relation $\Theta_s = B^{-\top} B_s B^{-1}$, we have

$$(\Theta_s v, v) = (B_s B^{-1} v, B^{-1} v);$$

hence, according to (2.8),

$$(\Theta_s v, v) \geqslant \frac{1}{2}\|\mathcal{T}^{-1}B^{-1}v\|^2. \tag{2.17}$$

We express the norm on the right-hand side as

$$\|\mathcal{T}^{-1}B^{-1}v\|^2 = \big(B^{-\top}\mathcal{T}^{-2}B^{-1}v,\, v\big) = \big(\mathcal{T}^{-1}B^{-\top}\mathcal{T}^{-2}B^{-1}\mathcal{T}^{-1}\mathcal{T}v,\, \mathcal{T}v\big)$$

and, following [6, (2.22)], introduce the positive definite, symmetric, tridiagonal matrix $D := \mathcal{T}B\mathcal{T}^2B^\top\mathcal{T}$, and easily see that

$$\|\mathcal{T}^{-1}B^{-1}v\|^2 = (D^{-1}\mathcal{T}v, \mathcal{T}v);$$

thus, (2.17) can be written in the form

$$(\Theta_s v, v) \geqslant \frac{1}{2}(D^{-1}\mathcal{T}v, \mathcal{T}v). \tag{2.18}$$

Now, assume for the time being that

$$(Dv, v) \leqslant 10\|v\|^2 \quad \forall v \in \mathbb{R}^n. \tag{2.19}$$

Then, obviously, $(D^{-1}v, v) \geqslant \|v\|^2/10$, and (2.18) yields the asserted property (2.16).

To prove (2.19), we first notice that the matrix D has the explicit form

$$D = \begin{pmatrix} 2d_0^{(1)} & d_1^{(2)} & & & 0 \\ d_1^{(2)} & 2d_0^{(2)} & d_1^{(3)} & & \\ & \ddots & \ddots & \ddots & \\ & & d_1^{(n-1)} & 2d_0^{(n-1)} & d_1^{(n)} \\ 0 & & & d_1^{(n)} & 2d_0^{(n)} \end{pmatrix},$$

where (with $r_1 := 0$ for simplicity)

$$2d_0^{(k)} = \Big(\frac{1+2r_k}{1+r_k}\Big)^2 + \frac{r_k^3}{(1+r_k)^2}, \quad d_1^{(k)} = -\frac{r_k^{\frac{3}{2}}}{1+r_k}\frac{1+2r_{k-1}}{1+r_{k-1}}, \quad k = 1, \dots, n.$$

Let $\psi(x) := \frac{(1+2x)^2}{(1+x)^2} + \frac{x^3}{(1+x)^2}$ and $\chi(x,y) := \frac{x^{3/2}}{1+x}\frac{1+2y}{1+y}$ for $x, y \in [0, r_\star]$. Since ψ, $\frac{x^{3/2}}{1+x}$, and $\frac{1+2y}{1+y}$ are increasing functions, by evaluating them at the upper bound $x = y = r_\star = 1+\sqrt{2}$, we obtain the estimates

$$2d_0^{(k)} \leqslant \psi(r_\star) \approx 4.1213 \quad \text{and} \quad |d_1^{(k)}| \leqslant \chi(r_\star, r_\star) \approx 1.87557,$$

and thus

$$2d_0^{(k)} + \frac{2}{5}|d_1^{(k)}| < 5 \quad \text{and} \quad \frac{5}{2}|d_1^{(k)}| < 5.$$

Therefore, applying the binomial inequality $2|v_kv_{k-1}| \leqslant 2v_k^2/5 + 5v_{k-1}^2/2$, we obtain

$$(Dv, v) = 2\sum_{k=2}^n (d_0^{(k)}v_k^2 + d_1^{(k)}v_kv_{k-1}) + 2d_0^{(1)}v_1^2 \leqslant 5\sum_{k=2}^n (v_k^2 + v_{k-1}^2) + 5v_1^2 \leqslant 10\|v\|^2,$$

i.e., (2.19). The proof is complete. $\square$

Notice that (2.15) can be written in the form

$$2\sum_{k=1}^{n} v_k \sum_{i=1}^{k} \theta_{k-i}^{(k)} v_i \geqslant \frac{1}{10}\sum_{k=1}^{n} \tau_k v_k^2, \quad n = 1,\dots,N. \tag{2.20}$$

We summarize properties of the DOC and DCC kernels that are required for our analysis in the following lemma.

Lemma 2.3 ([14,18])**.** *The DOC kernels* $\theta_i^{(n)}$ *and the DCC kernels* $p_i^{(n)}$ *satisfy the properties*

$$\theta_{n-i}^{(n)} > 0, \quad i = 1,\dots,n, \quad \textit{and} \quad \sum_{i=1}^{n} \theta_{n-i}^{(n)} = \tau_n, \quad n = 1,\dots,N, \tag{2.21}$$

$$p_{n-k}^{(n)} = \frac{1+r_k}{1+2r_k}\sum_{j=k}^{n} \tau_j \prod_{i=k+1}^{j} \frac{r_i}{1+2r_i}, \quad k = 1,\dots,n, \quad n = 1,\dots,N, \tag{2.22}$$

with $r_1 := 0$ *and* $\prod_{i=j+1}^{k} x_i = 1$ *for* $j \geqslant k$.

2.3. **An estimate for the DCC kernels $p_i^{(n)}$.** In the next lemma, we establish a new estimate for the DCC kernels, namely that $p_{n-k}^{(n)}$ is of the order of the current time step size τ_k, rather than of the maximum step size, in contrast to [18]. Estimate (2.23) plays a key role in the proof of Theorem 1.1 under our sharp ratio condition $r_i \leqslant r^\star < 1+\sqrt{2}$.

Lemma 2.4 (A crucial estimate for $p_{n-k}^{(n)}$)**.** *Under the ratio condition* $r_i \leqslant r^\star < 1+\sqrt{2}$*, the DCC kernel* $p_{n-k}^{(n)}$ *is bounded by the current time step size* τ_k*, that is,*

$$p_{n-k}^{(n)} \leqslant C_\star \tau_k, \quad k = 1,\dots,n, \quad n = 1,\dots,N, \tag{2.23}$$

with $C_\star := (1+2r^\star)/(1+2r^\star-(r^\star)^2)$.

Proof. Obviously $\prod_{i=k+1}^{j} r_i = \tau_j/\tau_k$; thus, it follows from (2.22) that the DCC kernel $p_{n-k}^{(n)}$ can be represented in the form

$$p_{n-k}^{(n)} = \frac{1+r_k}{1+2r_k}\tau_k \sum_{j=k}^{n} \prod_{i=k+1}^{j} \frac{r_i^2}{1+2r_i}, \quad k = 1,\dots,n. \tag{2.24}$$

Since $r_i \leqslant r^\star < 1+\sqrt{2}$, we have $\frac{r_i^2}{1+2r_i} \leqslant \frac{(r^\star)^2}{1+2r^\star} < 1$, and thus

$$p_{n-k}^{(n)} \leqslant \tau_k \sum_{j=k}^{n} \left(\frac{(r^\star)^2}{1+2r^\star}\right)^{j-k} \leqslant \frac{1+2r^\star}{1+2r^\star-(r^\star)^2}\tau_k. \qquad \square$$

Remark 2.1 (Sharpness of the ratio condition in Lemma 2.4)**.** If $r_i \geqslant 1+\sqrt{2}$ for all i in Lemma 2.4, then $r_i^2/(1+2r_i) \geqslant 1$, and (2.24) yields

$$p_{n-k}^{(n)} \geqslant \frac{1}{2}(n+1-k)\tau_k.$$

Keeping k fixed and letting n tend to ∞, we see that (2.23) is not satisfied. Hence, the bound on $r^\star$ in the ratio condition in Lemma 2.4 can not be relaxed.

2.4. **A discrete Gronwall-type inequality.** We give here a discrete Gronwall-type inequality that will be useful in the stability proof; see [6, Lemma 2.7].

Lemma 2.5 (A Gronwall-type inequality)**.** *Let C and $\alpha_i, x_i, y_i, i = 1, \dots, N$, be nonnegative numbers. If*

$$x_n^2 + y_n \leqslant C + \sum_{i=1}^{n} \alpha_i x_i, \quad n = 1, \dots, N, \tag{2.25}$$

then we have the estimate

$$x_n^2 + y_n \leqslant 2C + 2\Big(\sum_{i=1}^{n} \alpha_i\Big)^2, \quad n = 1, \dots, N. \tag{2.26}$$

Proof. Let

$$v_0 := C \quad \text{and} \quad v_n := C + \sum_{i=1}^{n} \alpha_i x_i, \quad n = 1, \dots, N.$$

Obviously, $v_n = v_{n-1} + \alpha_n x_n$. Hence, since in view of (2.25) $x_n^2 \leqslant v_n$, we have

$$v_n \leqslant v_{n-1} + \alpha_n \sqrt{v_n}, \quad n = 1, \dots, N.$$

Writing this inequality in the equivalent form

$$\Big(\sqrt{v_n} - \frac{\alpha_n}{2}\Big)^2 \leqslant \Big(\sqrt{v_{n-1}} + \frac{\alpha_n}{2}\Big)^2 - \alpha_n \sqrt{v_{n-1}},$$

we easily see that it implies

$$\sqrt{v_n} \leqslant \sqrt{v_{n-1}} + \alpha_n, \quad n = 1, \dots, N.$$

Therefore, we have

$$\sqrt{v_n} \leqslant \sqrt{v_0} + \sum_{i=1}^{n} \alpha_i = \sqrt{C} + \sum_{i=1}^{n} \alpha_i$$

and thus

$$v_n \leqslant 2C + 2\Big(\sum_{i=1}^{n} \alpha_i\Big)^2, \quad n = 1, \dots, N.$$

This result implies the asserted inequality (2.26) since, in view of (2.25), we have $x_n^2 + y_n \leqslant v_n$. □

3. Proof of Theorem 1.1

For $k \geqslant 2$, we consider the BDF method (1.2) with i instead of n, multiply it by $\theta_{k-i}^{(k)}$, and sum over i from $i = 2$ to $i = k$, and obtain

$$\sum_{i=2}^{k} \theta_{k-i}^{(k)} \dot{u}^i + \sum_{i=2}^{k} \theta_{k-i}^{(k)} A u^i = \sum_{i=2}^{k} \theta_{k-i}^{(k)} f^i. \tag{3.1}$$

We add the term $\theta_{k-1}^{(k)} \dot{u}^1$ to both sides, take advantage of relation (2.6), and write (3.1) as

$$u^k - u^{k-1} + \sum_{i=2}^{k} \theta_{k-i}^{(k)} A u^i = \sum_{i=2}^{k} \theta_{k-i}^{(k)} f^i + \theta_{k-1}^{(k)} \dot{u}^1. \tag{3.2}$$

Now, we shall use the energy technique. Testing (3.2) by $2u^k$ and summing over k from $k=2$ to $k=n$, we obtain

$$\begin{aligned} &2\sum_{k=2}^{n}(u^k-u^{k-1},u^k)+2\sum_{k=2}^{n}\sum_{i=2}^{k}\theta_{k-i}^{(k)}\langle u^i,u^k\rangle \\ &\quad=2\sum_{k=2}^{n}\sum_{i=2}^{k}\theta_{k-i}^{(k)}(f^i,u^k)+2\sum_{k=2}^{n}\theta_{k-1}^{(k)}(\dot u^1,u^k). \end{aligned} \tag{3.3}$$

First, we shall estimate the terms on the left-hand side of (3.3) from below. For the first term, we have

$$2\sum_{k=2}^{n}(u^k-u^{k-1},u^k)=\sum_{k=2}^{n}\big[|u^k|^2-|u^{k-1}|^2+|u^k-u^{k-1}|^2\big]\geqslant\sum_{k=2}^{n}\big[|u^k|^2-|u^{k-1}|^2\big],$$

whence

$$2\sum_{k=2}^{n}(u^k-u^{k-1},u^k)\geqslant|u^n|^2-|u^1|^2. \tag{3.4}$$

For the second term, we use (2.20) (with $v_1=0$), and obtain

$$2\sum_{k=2}^{n}\sum_{i=2}^{k}\theta_{k-i}^{(k)}\langle u^i,u^k\rangle\geqslant\frac{1}{10}\sum_{k=2}^{n}\tau_k\|u^k\|^2. \tag{3.5}$$

In view of (3.4) and (3.5), (3.3) yields

$$|u^n|^2+\frac{1}{10}\sum_{k=2}^{n}\tau_k\|u^k\|^2\leqslant|u^1|^2+2\sum_{k=2}^{n}\sum_{i=2}^{k}\theta_{k-i}^{(k)}(f^i,u^k)+2\sum_{k=2}^{n}\theta_{k-1}^{(k)}(\dot u^1,u^k). \tag{3.6}$$

Now, we shall show that the second term on the right-hand side of (3.6) can be estimated in the form

$$2\sum_{k=2}^{n}\sum_{i=2}^{k}\theta_{k-i}^{(k)}(f^i,u^k)\leqslant\frac{1}{20}\sum_{k=2}^{n}\tau_k\|u^k\|^2+20C_\star\sum_{i=2}^{n}\tau_i\|f^i\|_\star^2 \tag{3.7}$$

with $C_\star$ the constant of Lemma 2.4; we recall that the coefficients $\theta_{k-i}^{(k)}$ are positive. Indeed, first, obviously,

$$2(f^i,u^k)\leqslant2\|f^i\|_\star\|u^k\|\leqslant\frac{1}{20}\|u^k\|^2+20\|f^i\|_\star^2,$$

whence

$$2\sum_{k=2}^{n}\sum_{i=2}^{k}\theta_{k-i}^{(k)}(f^i,u^k)\leqslant\frac{1}{20}\sum_{k=2}^{n}\sum_{i=2}^{k}\theta_{k-i}^{(k)}\|u^k\|^2+20\sum_{k=2}^{n}\sum_{i=2}^{k}\theta_{k-i}^{(k)}\|f^i\|_\star^2. \tag{3.8}$$

For the first term on the right-hand side, we notice that

$$\sum_{i=2}^{k}\theta_{k-i}^{(k)}<\tau_k;$$

see (2.21). For the second term, using first (2.7) and subsequently (2.23), we have

$$\sum_{k=2}^{n}\sum_{i=2}^{k}\theta_{k-i}^{(k)}\|f^i\|_\star^2=\sum_{i=2}^{n}\sum_{k=i}^{n}\theta_{k-i}^{(k)}\|f^i\|_\star^2=\sum_{i=2}^{n}p_{n-i}^{(n)}\|f^i\|_\star^2\leqslant C_\star\sum_{i=2}^{n}\tau_i\|f^i\|_\star^2.$$

We infer that (3.8) yields the asserted estimate (3.7).

Now, from (3.6) and (3.7), we obtain

$$|u^n|^2+\frac{1}{20}\sum_{k=2}^n\tau_k\|u^k\|^2\leqslant|u^1|^2+20C_\star\sum_{i=2}^n\tau_i\|f^i\|_\star^2+2\sum_{k=2}^n\theta_{k-1}^{(k)}|\dot u^1||u^k|.$$

Utilizing here Lemma 2.5, we infer that

$$|u^n|^2+\frac{1}{20}\sum_{k=2}^n\tau_k\|u^k\|^2\leqslant 2|u^1|^2+40C_\star\sum_{i=2}^n\tau_i\|f^i\|_\star^2+8\Big(\sum_{k=2}^n\theta_{k-1}^{(k)}\Big)^2|\dot u^1|^2. \tag{3.9}$$

Furthermore, in view of (2.7) and (2.23), we have

$$\sum_{k=2}^n\theta_{k-1}^{(k)}\leqslant p_{n-1}^{(n)}\leqslant C_\star\tau_1,$$

and (3.9) yields

$$|u^n|^2+\frac{1}{20}\sum_{k=2}^n\tau_k\|u^k\|^2\leqslant 2|u^1|^2+40C_\star\sum_{i=2}^n\tau_i\|f^i\|_\star^2+8C_\star^2|u^1-u^0|^2.$$

This inequality immediately implies the asserted stability estimate (1.5); the proof of Theorem 1.1 is complete.

As in [3], [16, pp. 174–180], [8], and [1], we used the energy technique. Let us comment on some differences in these approaches. In [3], [16], and [8], (1.2) was tested by linear combinations of u^n and u^{n-1}, while linear combinations of u^n, u^{n-1}, and u^{n-2} were used in [1], in both cases with suitable coefficients. In [3], [16], [8], the terms were estimated at every time level and then were summed, whereas in [1] the relations were first summed and subsequently the sums were estimated. In contrast to these approaches, here, we first multiplied the method by suitable coefficients and summed to obtain (3.1), then tested by u^k, and summed again to get (3.3), before proceeding to estimate the sums.

The analysis in [10] is in the framework of Banach spaces and it is based on the Dunford–Taylor integral representation of certain functions of the operator A and on resolvent estimates. In [11], in Hilbert spaces, the method is written as a one-step scheme for pairs of consecutive approximations, $(u^{n-2},u^{n-1})\mapsto(u^{n-1},u^n)$; under the ratio condition $r_i\leqslant(1+\sqrt{3})/2$, it is shown that this mapping is contractive.

4. Nonautonomous equations

In this section, we use the stability result of Theorem 1.1 to establish stability of the variable two-step BDF method for nonautonomous equations under the same step ratio condition, $r_i\leqslant r^\star<1+\sqrt{2}$.

We consider the initial value problem

$$\begin{cases}u'(t)+A(t)u(t)=f(t), & 0<t<T,\\ u(0)=u_0,\end{cases} \tag{4.1}$$

with positive definite, selfadjoint, bounded operators $A(t):V\to V'$, $t\in[0,T]$.

For concreteness, we define the norm on V in terms of $A(0)$, i.e., $\|v\|:=|A(0)^{1/2}v|$. Our structural assumptions are that all operators $A(t), t\in[0,T]$, share the same domain, produce equivalent norms on V,

$$|A(t)^{1/2}v|\leqslant c|A(\tilde t)^{1/2}v|\quad\forall t,\tilde t\in[0,T]\ \ \forall v\in V, \tag{4.2}$$

and $A(t) : V \to V'$ is of bounded variation with respect to t,

$$|A(s)^{-1/2}\big(A(t) - A(\tilde t)\big)v| \leqslant [\sigma(t) - \sigma(\tilde t)]|A(s)^{1/2}v|,\ 0 \leqslant \tilde t \leqslant t \leqslant T,\ \forall v \in V, \tag{4.3}$$

for every $s \in [0, T]$, with an increasing function $\sigma : [0, T] \to \mathbb{R}$.

Clearly, $c \geqslant 1$ in (4.2), and the analogue of (4.2) holds true also for the dual norms $|A(t)^{-1/2}\cdot|$ on V' with the same constant c. Let us also note that (4.3) takes the form

$$\|\big(A(t) - A(\tilde t)\big)v\|_\star \leqslant [\sigma(t) - \sigma(\tilde t)]\|v\|, \quad 0 \leqslant \tilde t \leqslant t \leqslant T, \quad \forall v \in V,$$

for $s = 0$. Furthermore, if (4.3) is valid for a fixed $s \in [0, T]$, then, in view of (4.2), it is valid for any $s \in [0, T]$ with the right-hand side, that is with σ, multiplied by c^2.

Now, the variable two-step BDF method for the initial value problem (4.1) is

$$\dot u^n + A(t_n)u^n = f^n, \quad n = 2, \dots, N, \tag{4.4}$$

assuming that starting approximations $u^0, u^1 \in H$ are given. The next theorem provides a stability estimate of the scheme (4.4).

Theorem 4.1 (Stability of the variable two-step BDF method for nonautonomous equations)**.** *Let $u^0, u^1 \in H$. Assume that the time-dependent, positive definite, selfadjoint operators $A(t) : V \to V', t \in [0, T]$, satisfy the conditions (4.2) and (4.3). Then, the variable two-step BDF method (4.4) is stable, under the step ratio condition $r_i \leqslant r^\star < 1 + \sqrt{2}$, in the sense that*

$$|u^n|^2 + \sum_{\ell=2}^n \tau_\ell \|u^\ell\|^2 \leqslant \widetilde C\big(|u^0|^2 + |u^1|^2\big) + \widetilde C \sum_{\ell=2}^n \tau_\ell \|f^\ell\|_\star^2, \quad n = 2, \dots, N. \tag{4.5}$$

Here, $\widetilde C$ is a constant independent of $s, A(t)$, of the partition, and of n, that depends on $r^\star$, on σ, and exponentially on T.

Proof. Let us fix an $m, 2 \leqslant m \leqslant N$. From (4.4), we obtain

$$\dot u^n + A(t_m)u^n = g^{m,n} := [A(t_m) - A(t_n)]u^n + f^n, \quad n = 2, \dots, m.$$

Since the time t is frozen at t_m in the operator $A(t_m)$ on the left-hand side, we can apply the already-established stability estimate (1.5), for the time-independent operator $A := A(t_m)$, and obtain

$$|u^m|^2 + \sum_{\ell=2}^m \tau_\ell |A(t_m)^{1/2}u^\ell|^2 \leqslant C\big(|u^0|^2 + |u^1|^2\big) + C\sum_{\ell=2}^m \tau_\ell |A(t_m)^{-1/2}g^{m,\ell}|^2 \tag{4.6}$$

with a constant C independent of m. By the triangle inequality,

$$|A(t_m)^{-1/2}g^{m,\ell}| \leqslant |A(t_m)^{-1/2}[A(t_m) - A(t_\ell)]u^\ell| + |A(t_m)^{-1/2}f^\ell|,$$

and, in view of the bounded variation condition (4.3), we have

$$|A(t_m)^{-1/2}g^{m,\ell}| \leqslant [\sigma(t_m) - \sigma(t_\ell)]|A(t_m)^{1/2}u^\ell| + |A(t_m)^{-1/2}f^\ell|.$$

Therefore, using (4.2) and its analogue for the dual norms, we infer from (4.6) that

$$|u^m|^2 + \sum_{\ell=2}^m \tau_\ell \|u^\ell\|^2 \leqslant C_1 G_m + C_1\Big(|u^0|^2 + |u^1|^2 + \sum_{\ell=2}^m \tau_\ell \|f^\ell\|_\star^2\Big) \tag{4.7}$$

with the constant $C_1 := 2c^4C$ and

$$G_m := \sum_{\ell=2}^{m} \tau_\ell [\sigma(t_m) - \sigma(t_\ell)]^2 \|u^\ell\|^2.$$

It remains to prove that G_m is dominated by the second term on the right-hand side of (4.7); then, estimate (4.5) follows immediately from (4.7).

Letting

$$E_1 := 0, \quad E_\ell := \sum_{i=2}^{\ell} \tau_i \|u^i\|^2, \quad \ell = 2, \dots, m,$$

and employing summation by parts, we rewrite G_m in the form

$$G_m = \sum_{\ell=2}^{m-1} \big[\sigma(t_m) - \sigma(t_\ell)\big]^2 (E_\ell - E_{\ell-1}) = \sum_{\ell=2}^{m-1} a_{m,\ell} E_\ell \tag{4.8}$$

with $a_{m,\ell} := \big[\sigma(t_m) - \sigma(t_\ell)\big]^2 - \big[\sigma(t_m) - \sigma(t_{\ell+1})\big]^2 \geqslant 0, \ell = 2, \dots, m-1$.

Inserting (4.8) into (4.7) and estimating the term on the left-hand side from below by E_m, we obtain

$$E_m \leqslant C_1 \sum_{\ell=2}^{m-1} a_{m,\ell} E_\ell + C_1 \Big(|u^0|^2 + |u^1|^2 + \sum_{\ell=2}^{m} \tau_\ell \|f^\ell\|_\star^2 \Big). \tag{4.9}$$

With $M := \sigma(T) - \sigma(0)$ the total variation of σ, we have

$$a_{m,\ell} = \big[\sigma(t_{\ell+1}) - \sigma(t_\ell)\big]\big[2\sigma(t_m) - \sigma(t_\ell) - \sigma(t_{\ell+1})\big] \leqslant 2M\big[\sigma(t_{\ell+1}) - \sigma(t_\ell)\big],$$

and infer from (4.9) that

$$E_m \leqslant \widetilde{C}_1 \sum_{\ell=2}^{m-1} \big[\sigma(t_{\ell+1}) - \sigma(t_\ell)\big] E_\ell + C_1 \Big(|u^0|^2 + |u^1|^2 + \sum_{\ell=2}^{m} \tau_\ell \|f^\ell\|_\star^2 \Big), \quad m = 2, \dots, N,$$

with $\widetilde{C}_1 := 2MC_1$. Therefore, a standard discrete Gronwall-type argument leads to

$$E_m \leqslant C_2 \Big(|u^0|^2 + |u^1|^2 + \sum_{\ell=2}^{m} \tau_\ell \|f^\ell\|_\star^2 \Big), \quad m = 2, \dots, N. \tag{4.10}$$

Finally, since the sequence (E_ℓ) is increasing, (4.8) yields

$$G_m \leqslant E_m \sum_{\ell=2}^{m-1} a_{m,\ell} = E_m \big[\sigma(t_m) - \sigma(t_2)\big]^2 \leqslant M^2 E_m.$$

Combining this estimate with (4.10), we deduce that G_m is indeed dominated by the second term on the right-hand side of (4.7), and the proof of the asserted stability estimate (4.5) for the case of nonautonomous equations is complete. $\square$

5. Numerical Experiments

In this section, we present results of numerical experiments designed to evaluate the performance of the variable two-step BDF scheme (1.2) under various parameter configurations. Specifically, we examine the boundedness of the numerical approximations for various step-size ratios.

5.1. **Verification for a scalar test equation.** We apply the variable two-step BDF scheme to a test equation, employing a fixed step-size ratio $r_i = r > 1$. The time steps are defined by $\tau_n := \frac{(r-1)r^{n-1}}{r^N-1}T$, where N represents the total number of time steps.

Example 5.1. Consider an initial value problem for a test equation,

$$u' + u = 0, \quad t > 0, \quad u(0) = 1. \tag{5.1}$$

TABLE 5.1. Numerical approximations u^N at $T = 10$ for two step-size ratios (Example 5.1).

N	$\lvert u^N\rvert$, $r = 2.4$	$\lvert u^N\rvert$, $r = 2.5$
50	$6.8285 \cdot 10^{-2}$	$7.7166 \cdot 10^{-2}$
100	$6.8306 \cdot 10^{-2}$	$7.7986 \cdot 10^{-2}$
200	$6.8331 \cdot 10^{-2}$	$1.3292 \cdot 10^{-1}$
400	$6.8350 \cdot 10^{-2}$	$1.9640 \cdot 10^{2}$

Numerical simulations reveal a clear phase transition from bounded numerical approximations to exponentially increasing approximations as the step-size ratio r increases. To systematically pinpoint the critical value of this transition, we introduce a controlled perturbation 10^{-5} into the second starting approximation u^1. So, we implemented the variable two-step BDF method with starting values $u^0 = 1$ and $u^1 = \exp(-\tau_1) + 10^{-5}$. The results in Table 5.1 clearly demonstrate a sharp contrast in the behavior of the numerical approximations across the theoretical threshold $r = 1 + \sqrt{2}$. For $r < 1 + \sqrt{2}$, the numerical approximations remain bounded and well-controlled. In contrast, for $r \geqslant 1 + \sqrt{2}$, the approximations rapidly increase. This observation shows excellent agreement with and thereby verifies our theoretical analysis in Theorem 1.1.

5.2. **Verification for parabolic equations.** We now extend our analysis to a prototypical parabolic p.d.e. Let $\Omega = (0,1)^2 \subset \mathbb{R}^2$ and $T > 0$. We consider the initial boundary value problem

$$\begin{cases} u_t - \nabla \cdot (\mathcal{Q}\nabla u) = f & \text{in } \Omega \times (0,T], \\ u = 0 & \text{on } \partial\Omega \times (0,T], \\ u(\cdot,0) = u_0 & \text{in } \Omega. \end{cases} \tag{5.2}$$

Here, the diffusion coefficient $\mathcal{Q} : \Omega \times [0,T] \to \mathbb{R}^{2,2}$ is a time-dependent, symmetric matrix-valued function. The forcing term $f : \Omega \times [0,T] \to \mathbb{R}$ and the initial value $u_0 : \Omega \to \mathbb{R}$ will be specified according to the exact solutions introduced later.

5.2.1. *Full discretization.* In space we discretize by conforming finite elements. We use a uniform triangular partition of the domain Ω, and let the finite element space S_h^3 be

$$S_h^3 := \left\{ v \in H_0^1(\Omega) \;\middle|\; v|_K \in \mathbb{P}_3(K),\ \forall K \in \mathcal{T}_h \right\};$$

here, $\mathbb{P}_3(K)$ denotes the space of bivariate polynomials of total degree at most 3 in an element K, and $H_0^1(\Omega)$ enforces the homogeneous Dirichlet boundary condition.

We use the variable two-step BDF method for time stepping. So, given starting approximations $u_h^0, u_h^1 \in S_h^3$, we define fully discrete approximations $u_h^n \in S_h^3, n = 2, \dots, N$, to the nodal values $u(\cdot, t_n)$ by

$$(\dot{u}_h^n, v_h) + (\mathcal{a}_h^n \nabla u_h^n, \nabla v_h) = (f_h^n, v_h) \quad \forall v_h \in S_h^3,$$

where u_h^0, $\mathcal{a}_h^n$, and f_h^n are the finite element interpolants of $u(\cdot, t_0)$, $\mathcal{a}(\cdot, t_n)$, and $f(\cdot, t_n)$, respectively. A spatial discretization parameter of $h = 1/40$ is adopted to ensure that the temporal error remains dominant. We use a fixed step-size ratio r. The method is initialized by employing a single step of the implicit Euler scheme.

5.2.2. *Numerical results.*

Example 5.2. We first consider a test case with a constant, isotropic diffusion coefficient, $\mathcal{a}(\boldsymbol{x}, t) = I_2$, with I_2 the 2×2 identity matrix, i.e., the heat equation,

$$u_t - \varDelta u = f.$$

The exact solution is manufactured as

$$u(\boldsymbol{x}, t) = \mathrm{e}^{-t} \sin(\pi x) \sin(\pi y).$$

The L^2-norms, $|\cdot|$, of the numerical approximations u^N at $T = 1$, for two step-size ratios, are displayed in Table 5.2. The results demonstrate a critical dependence on r. For $r = 2$, the approximations remain stable and controlled as the number of time steps N increases. In sharp contrast, for $r = 4$, the approximations exhibit rapid growth, leading to a complete blow-up upon grid refinement.

Table 5.2. The L^2-norms, $|\cdot|$, of the numerical approximations u^N at $T = 1$ for two step-size ratios (Example 5.2).

N	$\lvert u^N\rvert, \quad r = 2$	$\lvert u^N\rvert, \quad r = 4$
16	$1.8320 \cdot 10^{-1}$	$1.8240 \cdot 10^{-1}$
32	$1.8320 \cdot 10^{-1}$	$1.8240 \cdot 10^{-1}$
64	$1.8320 \cdot 10^{-1}$	$1.9818 \cdot 10^{-1}$
128	$1.8320 \cdot 10^{-1}$	$1.5710 \cdot 10^{14}$
256	$1.8320 \cdot 10^{-1}$	$1.5153 \cdot 10^{46}$

Up to this point, all step-size ratios either satisfied or violated the ratio condition (1.4). Next, we examine a scenario where the ratio condition (1.4) is violated in a specific sense, namely, a fixed number $n^\star$ of ratios r_i exceed the upper bound $1 + \sqrt{2}$, more precisely, are equal to 5, while $N - n^\star - 1$ ratios r_i are equal to 2.4, and thus less than the upper bound. The corresponding numerical results are displayed in Table 5.3. Notably, despite the fact that the ratio condition (1.4) is violated in this specific sense, the approximations remain uniformly bounded.

Example 5.3. We further investigate the performance of the method under a more challenging scenario featuring a time-dependent and anisotropic diffusion coefficient,

$$\mathcal{a}(\boldsymbol{x}, t) = \begin{pmatrix} 1 + \mu & t \\ t & 1 + \mu \end{pmatrix}, \quad 0 \leqslant t \leqslant 1,$$

TABLE 5.3. The L^2-norms, $|\cdot|$, of the numerical approximations u^N at $T = 1$ when only $n^\star$ ratios r_i exceed the upper bound in (1.4) (Example 5.2).

N	$\lvert u^N\rvert,\ n^\star = 10$	$\lvert u^N\rvert,\ n^\star = 20$
40	$1.82286 \cdot 10^{-1}$	$1.82225 \cdot 10^{-1}$
80	$1.82505 \cdot 10^{-1}$	$1.82668 \cdot 10^{-1}$
160	$1.82949 \cdot 10^{-1}$	$1.82932 \cdot 10^{-1}$
320	$1.82932 \cdot 10^{-1}$	$1.82840 \cdot 10^{-1}$
640	$1.82949 \cdot 10^{-1}$	$1.82949 \cdot 10^{-1}$

with a constant $\mu > 0$ ensuring uniform coercivity. The exact solution is prescribed as

$$u(\boldsymbol{x}, t) = \mathrm{e}^t \sin(\pi x) \sin(\pi y).$$

We set the final time $T = 1$ and examine two cases, $\mu = 0.1$ and $\mu = 0.5$, to probe the influence of the properties of the diffusion operator on the numerical stability. The corresponding results are presented in Tables 5.4 and 5.5, respectively.

The results in Tables 5.4 and 5.5 provide a clear numerical validation of our theoretical analysis. First, the critical transition from bounded approximations to blow-up occurs around $r = 1+\sqrt{2}$, which is in full agreement with Theorem 4.1. The bounded approximations for $r = 2$ and $r = 2.4$ exhibit remarkable stability under temporal refinement, while a sharp contrast is observed for $r = 3$ and $r = 4$, where the approximations explode catastrophically. Second, for a variable-coefficient matrix $\mathcal{Q}$ satisfying the assumptions in Theorem 4.1, the numerical approximations remain bounded, thus corroborating the theoretical stability conditions. Notably, the stronger diffusion, $\mu = 0.5$, delays the onset of instability compared to the weaker case, $\mu = 0.1$, confirming that the stability is intrinsically linked to the properties of the diffusion operator as stipulated by the theory.

TABLE 5.4. The L^2-norms, $|\cdot|$, of the numerical approximations u^N at $T = 1$ for various step-size ratios for $\mu = 0.1$ (Example 5.3).

N	$\lvert u^N\rvert,\ r = 2$	$\lvert u^N\rvert,\ r = 2.4$	$\lvert u^N\rvert,\ r = 3$	$\lvert u^N\rvert,\ r = 4$
40	$1.36215 \cdot 10^{0}$	$1.36289 \cdot 10^{0}$	$1.36362 \cdot 10^{0}$	$1.36432 \cdot 10^{0}$
80	$1.36215 \cdot 10^{0}$	$1.36289 \cdot 10^{0}$	$1.36362 \cdot 10^{0}$	$1.95707 \cdot 10^{2}$
160	$1.36215 \cdot 10^{0}$	$1.36289 \cdot 10^{0}$	$9.55658 \cdot 10^{0}$	$1.88233 \cdot 10^{22}$
320	$1.36215 \cdot 10^{0}$	$1.36289 \cdot 10^{0}$	$1.47732 \cdot 10^{18}$	$1.79925 \cdot 10^{62}$

Example 5.4. Here, we consider the heat equation in an L-shaped domain Ω,

$$\Omega = (-1, 1)^2 \setminus \big([0, 1) \times (-1, 0]\big),$$

subject to mixed boundary conditions, to interstage the performance of the method in more complex situations. More precisely, we impose Robin boundary conditions

$$u_y + u = g_{\mathrm{Robin}}$$

TABLE 5.5. The L^2-norms, $|\cdot|$, of the numerical approximations u^N at $T=1$ for various step-size ratios for $\mu=0.5$ (Example 5.3).

N	$\lvert u^N\rvert,\quad r=2$	$\lvert u^N\rvert,\ r=2.4$	$\lvert u^N\rvert,\quad r=3$	$\lvert u^N\rvert,\quad r=4$
40	$1.36124\cdot 10^{0}$	$1.36175\cdot 10^{0}$	$1.36225\cdot 10^{0}$	$1.36273\cdot 10^{0}$
80	$1.36124\cdot 10^{0}$	$1.36175\cdot 10^{0}$	$1.36225\cdot 10^{0}$	$1.52175\cdot 10^{2}$
160	$1.36124\cdot 10^{0}$	$1.36175\cdot 10^{0}$	$5.51011\cdot 10^{0}$	$1.45924\cdot 10^{22}$
320	$1.36124\cdot 10^{0}$	$1.36175\cdot 10^{0}$	$7.46372\cdot 10^{17}$	$1.39484\cdot 10^{62}$

on the boundary segment $y=1$ and homogeneous Dirichlet boundary conditions on the remaining part of the boundary $\partial\Omega$. The exact solution and g_{Robin} are manufactured as follows

$$u(\boldsymbol{x},t)=\mathrm{e}^{-t}\,x(x^2-1)\,y(y+1),\quad g_{\text{Robin}}(x,1,t)=5\mathrm{e}^{-t}\,x(x^2-1).$$

Let us mention that no boundary conditions are imposed on the finite element spaces on the Robin part of the boundary.

Although our theory is not directly applicable in this case due to the inhomogeneous Robin boundary conditions, to further validate the performance of the method in this more complex setting, we considered four different ratios, $r=2,2.4,3,$ and 4. As shown in Table 5.6, the method is stable when our ratio condition is satisfied whereas instability occurs as the time grid is refined when the ratio condition is violated. This example confirms that the method behaves as expected when applied to problems with more complex geometries and mixed boundary conditions.

TABLE 5.6. The L^2-norms, $|\cdot|$, of the numerical approximations u^N at $T=1$ in an L-shaped domain with mixed boundary conditions (Example 5.4).

N	$\lvert u^N\rvert,\quad r=2$	$\lvert u^N\rvert,\ r=2.4$	$\lvert u^N\rvert,\quad r=3$	$\lvert u^N\rvert,\quad r=4$
40	$1.46399\cdot 10^{-1}$	$1.46148\cdot 10^{-1}$	$1.45876\cdot 10^{-1}$	$1.45590\cdot 10^{-1}$
80	$1.46399\cdot 10^{-1}$	$1.46148\cdot 10^{-1}$	$1.45876\cdot 10^{-1}$	$5.41032\cdot 10^{1}$
160	$1.46399\cdot 10^{-1}$	$1.46148\cdot 10^{-1}$	$7.53998\cdot 10^{-1}$	$5.22003\cdot 10^{21}$
320	$1.46399\cdot 10^{-1}$	$1.46148\cdot 10^{-1}$	$4.87007\cdot 10^{18}$	$4.98964\cdot 10^{61}$

Example 5.5. In this example, we consider the homogeneous heat equation in the domain $\Omega=(0,1)^2$, subject to homogeneous Dirichlet boundary conditions, with rough initial data to further illustrate the practical benefit of the new stability bound. The initial value is a piecewise constant function,

$$u_0(x,y)=\begin{cases}1, & 0.4\leqslant x\leqslant 0.6,\quad 0.4\leqslant y\leqslant 0.6,\\ 0, & \text{otherwise.}\end{cases}$$

In the computation, we take the spatial mesh size $h=1/100$ and employ an adaptive variable-step two-step BDF scheme for time discretization; see [15]. The

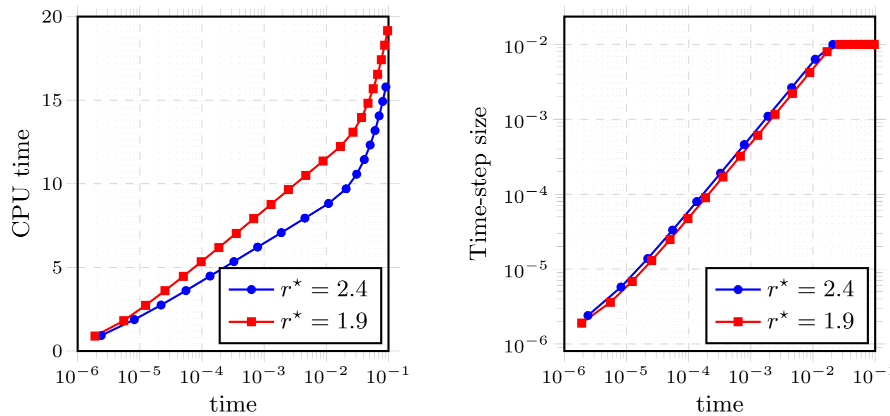

FIGURE 5.1. Accumulated CPU time (left) and time-step size (right) versus physical time, in seconds, for $T = 0.1$ (Example 5.5).

time steps are determined by

$$\tau_{n+1} := \min\Big\{r^\star\tau_n,\ \max\Big(\tau_{\min},\frac{\tau_{\max}}{\sqrt{1+\alpha|\bar\partial E^n|}}\Big)\Big\},$$

with $\tau_{\max} = 10^{-2}, \tau_{\min} = 10^{-6}, \alpha = 10^{-7}$, and

$$E^n = \int_\Omega |\nabla u^n|^2\,\mathrm{d}x, \quad \bar\partial E^n = (E^n - E^{n-1})/\tau_n.$$

The quantity $\bar\partial E^n$ is used as an energy-based indicator to adapt the time-step size.

We compare the performance of the method under the relaxed stability condition $r^\star < 1+\sqrt{2}$ and the mildest previously known condition $r^\star < 1.9398$ from [1]. Figure 5.1 (left) displays the accumulated CPU time versus the physical time, while Figure 5.1 (right) shows the corresponding time-step evolution. The results indicate that the improved ratio condition (1.4) enables a faster increase of the time-step size in the early stage of the computation, thereby improving the computational efficiency. In this test, the total CPU time is reduced by about 17.5%.

REFERENCES

[1] G. Akrivis, M. Chen, J. Han, F. Yu, and Z. Zhang, *The variable two-step BDF method for parabolic equations*, BIT Numer. Math. **64** (2024), Paper no. 14, 21 pp. DOI 10.1007/s10543-024-01007-y. MR4712451

[2] J. Becker, *A second order backward difference method with variable steps for a parabolic problem*, Reprint No. 1993-03, Department of Mathematics, Chalmers University of Technology, Göteborg, 1993.

[3] J. Becker, *A second order backward difference method with variable steps for a parabolic problem*, BIT **38** (1998) 644–662. DOI 10.1007/BF02510406. MR1670200

[4] W. Chen, X. Wang, Y. Yan, and Z. Zhang, *A second order BDF numerical scheme with variable steps for the Cahn-Hilliard equation*, SIAM J. Numer. Anal. **57** (2019) 495–525. DOI 10.1137/18M1206084. MR3916957

[5] M. Crouzeix and F. J. Lisbona, *The convergence of variable-stepsize, variable formula, multistep methods*, SIAM J. Numer. Anal. **21** (1984) 512–534. DOI 10.1137/0721037. MR744171

[6] Y. Di, Y. Ma, J. Shen, and J. Zhang, *A variable time-step IMEX-BDF2 SAV scheme and its sharp error estimate for the Navier–Stokes equations*, ESAIM Math. Model. Numer. Anal. **57** (2023) 1143–1170. DOI 10.1051/m2an/2023007. MR4584733

[7] Y. Di, Y. Wei, J. Zhang, and C. Zhao, *Sharp error estimate of an implicit BDF2 scheme with variable time steps for the phase field crystal model*, J. Sci. Comput. **92** (2022) 65. DOI 10.1007/s10915-022-01919-3. MR4450100

[8] E. Emmrich, *Stability and error of the variable two-step BDF for semilinear parabolic problems*, J. Appl. Math. Comput. **19** (2005) 33–55. DOI 10.1007/BF02935787. MR2162306

[9] R. D. Grigorieff, *Stability of multistep-methods on variable grids*, Numer. Math. **42** (1983) 359–377. DOI 10.1007/BF01389580. MR723632

[10] R. D. Grigorieff, *Time discretization of semigroups by the variable two-step BDF method*, in Numerical Treatment of Differential Equations, K. Strehmel, ed., (NUMDIFF-5, Halle 1989), Teubner-Texte zur Mathematik **121**, Stuttgart, 1991, pp. 204–216. MR1128354

[11] R. D. Grigorieff, *On the variable two-step BDF method for parabolic equations*, Preprint 426/1995, Institute of Mathematics, T.U. Berlin.

[12] E. Hairer, S. Nørsett, and G. Wanner, Solving Ordinary Differential Equations I: Nonstiff Problems. 2^{nd} ed., Springer–Verlag, Berlin, 1993. DOI 10.1007/978-3-540-78862-1. MR1227985

[13] H.-L. Liao, B. Ji, and L. Zhang, *An adaptive BDF2 implicit time-stepping method for the phase field crystal model*, IMA J. Numer. Anal. **42** (2022) 649–679. DOI 10.1093/imanum/draa075. MR4367667

[14] H.-l. Liao and Z. Zhang, *Analysis of adaptive BDF2 scheme for diffusion equations*, Math. Comp. **90** (2021) 1207–1226. DOI 10.1090/mcom/3585. MR4232222

[15] Z. Qiao, Z. Zhang, and T. Tang, *An adaptive time-stepping strategy for the molecular beam epitaxy models*, SIAM J. Sci. Comput. **33** (2011) 1395–1414. DOI 10.1137/100812781. MR2813245

[16] V. Thomée, Galerkin Finite Element Methods for Parabolic Problems, 2^{nd} ed., Springer–Verlag, Berlin, 2006. DOI 10.1007/3-540-33122-0. MR2249024

[17] W. Wang, M. Mao, and Z. Wang, *Stability and error estimates for the variable step-size BDF2 method for linear and semilinear parabolic equations*, Adv. Comput. Math. **47** (2021) 8. DOI 10.1007/s10444-020-09839-2. MR4206656

[18] J. Zhang and C. Zhao, *Sharp error estimate of BDF2 scheme with variable time steps for linear reaction-diffusion equations*, J. Math. (China) **41** (2021) 471–488. DOI 10.3969/j.issn.0255-7797.2021.01.002.

[19] J. Zhang and C. Zhao, *Sharp error estimate of BDF2 scheme with variable time steps for molecular beam epitaxial models without slope selection*, J. Math. (China) **42** (2022) 377–401. DOI 10.3969/j.issn.0255-7797.2022.05.001.

[20] C. Zhao, R. Yang, Y. Di, and J. Zhang, *Sharp error estimate of variable time-step IMEX BDF2 scheme for parabolic integro-differential equations with initial singularity arising in finance*, J. Comput. Math. **43** (2025) 1118–1140. DOI 10.4208/jcm.2406-m2023-0095. MR4969513

Department of Computer Science and Engineering, University of Ioannina, 451 10 Ioannina, Greece, and Institute of Applied and Computational Mathematics, FORTH, 700 13 Heraklion, Crete, Greece

Email address: akrivis@cse.uoi.gr

Department of Applied Mathematics, The Hong Kong Polytechnic University, Hung Hom, Kowloon, Hong Kong

Email address: yi-fan.wei@polyu.edu.hk

School of Mathematics and Statistics, and Hubei Key Laboratory of Computational Science, Wuhan University, Wuhan 430072, China

Email address: jiweizhang@whu.edu.cn

School of Mathematical Science, Eastern Institute of Technology, Ningbo, Zhejiang 315200, P. R. China

Email address: cczhao@eitech.edu.cn